Remote Sensing and GIS for Hydrology and Water Resources (IAHS Publ. 368, 2015)
(Proceedings RSHS14 and ICGRHWE14, Guangzhou, China, August 2014).

Application of ZY-3 remote sensing image in the research of Huashan experimental watershed

KUN GUO, JIANQUN WANG & YANG WANG
College of Hydrology and Water resources, Hohai University, Nanjing, Jiangsu Province, 210098, China
guokunhhu@163.com

Abstract Spatial information of Huashan experimental watershed, such as a DEM and land-use types, is extracted from ZY-3 images and studied for digital watershed construction and hydrological simulation. A high-accuracy DEM is extracted from the ZY-3 stereoscopic image. Water body information is extracted from high-accuracy fused images by the method of supervised classification with object-oriented techniques. Land-use types are extracted by the decision tree classification method based on mono-temporal fused image and multiple-temporal multispectral images. The construction of the classification decision tree of the mono-temporal images is based on a multivariate statistical analysis method and the construction of classification decision tree of the multiple-temporal images is based on the CART algorithm. The land-use information which meets the accuracy needs is synthesized into a final land-use map. The accuracy of the final land-use map was evaluated; the overall classification accuracy was 92.04% and the Kappa coefficient was 0.9030.

Key words ZY-3; remote sensing; hydrological experimental watershed; land use

1 INTRODUCTION

An experimental watershed is a desirable research object for hydrology, water resource and water environment and an important means to exploring the processes of hydrology, water resources and water environment systems under changing environments and looking for ways of sustainable utilization of water resources. Hydrological research on experimental watersheds has long been a part of the International Hydrological Program (Fu *et al*., 2011). The No.1 experimental watershed of the Chuzhou hydrological experimental station was built in 1978, and the Chuzhou hydrological experimental station was built in 1981. A number of basic research achievements and high-quality academic papers with substantial domestic and foreign influence have resulted from the research on the hydrological cycle, runoff mechanisms, soil water movement and isotope experimental observation technology based on Huashan hydrological experimental watershed of Chuzhou experimental station (Gu *et al*. 2003). To carry out research into pollutant migration mechanisms based on the experimental watershed, the digital watershed of Huashan experimental watershed is needed. ZY-3, which was successfully launched by CZ-4B Y26 at the Taiyuan Satellite Launch Center in January 2012, is China's first independently-developed high-resolution civil stereo mapping satellite. The satellite can achieve seamless image coverage for the area within 84 degrees north and south longitudes with a recursive period of 59 days and a revisit period of five days. As a new type of remote sensing image data source, the image data from ZY-3 has advantages such as high spatial resolution, large dynamic range and three-dimensional imaging. Consequently, the satellite data has a broad application potential such as in environmental protection, resource investigation and emergency relief, as well as wide application in the field of surveying and mapping (CRESDA 2013, Li *et al*. 2012).

In this paper, spatial information of Huashan hydrological experimental watershed is extracted from ZY-3 remote sensing images and studied for digital watershed construction and hydrological simulation. This study will gather experience for applying the remote sensing images from ZY-3 to the research on hydrological experimental watershed.

2 MATERIALS AND METHODS

Located in the area from 118°8′7″E to 118°16′51″E and from 32°13′15″N to 32°18′55″N, Huashan hydrological experimental watershed is in Chuzhou, Anhui Province, China. The watershed has a total area of 82.1 km^2. It has a complex hilly terrain with a mainly rural landscape, where farmland, small reservoirs and forestland also occur.

In this study, the image data covering the study area from ZY-3 include the following: multispectral images on 2 October 2012; panchromatic, multispectral (four bands) and forward-looking and backward-looking images on 28 January 2013; and multispectral images on 29 July 2013. These images were all provided by China Centre for Resources Satellite Data and Application (CRESDA). The remote sensing image processing platform is ENVI 4.8, and the modifying process is finished under the platform ArcGIS 9.2 after classification.

From the stereo images formed by forward-looking and backward-looking images of ZY-3 on 28 January 2013, the DEM of the study area is extracted. The spatial resolution of the DEM of the study area is 4 m (Fig. 1). Radiation calibration and atmospheric correction is conducted for multispectral images of different time phases and panchromatic images, respectively. Radiation calibration is carried out with calibration coefficients and calibration formulas provided by CRESDA (2013). The calibration coefficient is selected according to the corresponding year. According to the spectral response function provided by CRESDA (2013), the FLAASH method is adopted for atmospheric correction (Han *et al*. 2011). Ortho-rectification of remote sensing images is made by the RPC model of ZY-3 and the DEM. Multispectral images with different time phase and panchromatic image on 28 January 2013 were aggregated for image registration. These images are fused by the Gram-Schmidt method after image registration. Remote sensing images of the study area, as the study objective, are cut out from the images after fusion and the multispectral image with various time phases, respectively.

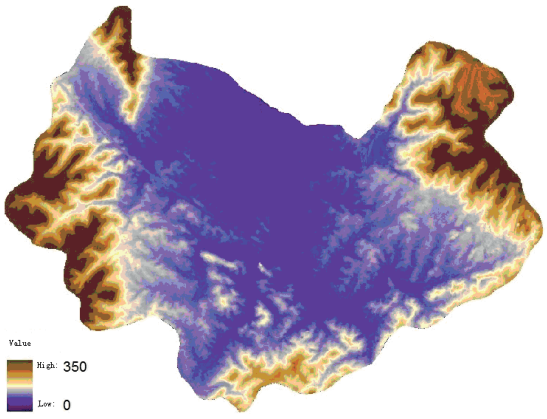

Fig. 1 DEM of Huashan Hydrological Experimental Watershed.

In light of the features of high-resolution remote sensing image, Baatz and Schape proposed the object-oriented remote sensing image classification method (Baatz and Schape 1999), and the core technology is multi-scale segmentation based on the heterogeneity minimum principle (object generation) and fuzzy mathematical analysis based on the fuzzy logic classification system (information extraction) (Metzler and Aact 2002). The main idea is to form a polygon object from homogeneous pixels after image segmentation, analyse the characteristics of the target land class attribute, and classify and extract the polygon object through fuzzy decision rules (Wu *et al.* 2013). This method takes full advantages of the characteristics of spectral colour, texture and shape reflected in remote sensing images to get the classification based on the polygon object, and varies from traditional classification methods based on pixels by making full use of the image geometric information and improves classification accuracy. Water body, as an important research object in hydrological experimental watersheds, requires high accuracy information on the location, number, size and contour in its scientific research. The object-oriented method is adopted to extract water information.

The classification rules are generated and the classification made by the decision tree classification method through a decision-making learning process. The classification samples are distribution free and need not meet a normal distribution. The decision tree classification method

could make full use of the geological knowledge in the GIS database to assist classification, and it improves classification accuracy significantly (Friedl *et al.* 1999). The decision tree classification method has been widely used in information extraction of various types of remote sensing images and land-use classification (Mclver and Friedl 2001, Mclver and Friedl 2002, Wei *et al*. 2010). In this paper, land-use types are extracted by the decision tree classification method based on mono-temporal fused image and multiple-temporal multispectral images, respectively. The construction of the classification decision tree of the mono-temporal images are based on a spectral analysis method and the construction of the classification decision tree of the multiple-temporal images is based on the CART algorithm (Chen *et al*. 2008).

The water information extracted by the object-oriented method, the land-use information extracted by the decision tree classification method based on mono-temporal fused image and the land-use information extracted by the decision tree classification method based on the multiple-temporal multispectral images, are optimally synthesized to get the final land-use map and the accuracy of the land-use map is evaluated.

In accordance with the characteristics of the landscape and research needs, the land cover types are finally divided into seven classes, namely paddy, upland, evergreen forest, deciduous forest, water body, building land and bare land.

3 INFORMATION EXTRACTION AND RESULT ANALYSIS

3.1 Extraction of land-use information

Among the remote sensing image data of the study area, there are only data of panchromatic images and the multi-spectral images on 28 January 2013. The spatial resolution of the image fused by the panchromatic image and the multi-spectral images is 2.1 m, much better than others. Therefore, the fused image is selected as a study object and segmented according to the image features of spectra, colour, texture and shape. Water body information is extracted based on the image spots by the supervision classification method. All of the water bodies obtained in the process of the experimental study are selected for examples of the supervision classification, and finally the water body information with high accuracy is obtained (Fig. 2).

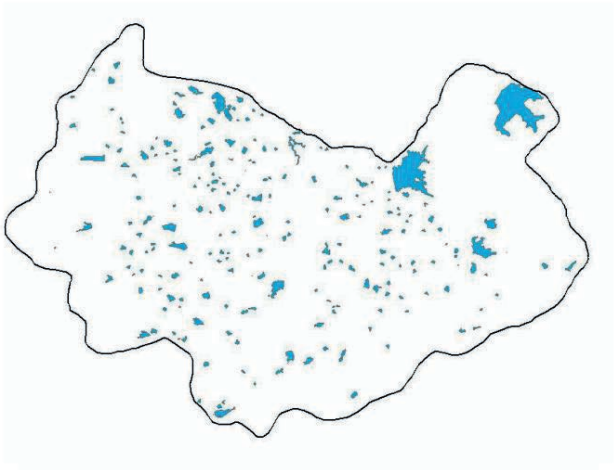

Fig. 2 Water bodies map.

The fused image on 28 January 2013 has the highest spatial resolution, and was also selected for mono-temporal image classification. The classification decision statistics of the final selection are NDWI, NDVI, SR, ARVI, B2 and JZZS. Here B2 is the second band (green band), JZZS represents statistics calculated from different responses of the first band (blue band) and the fourth band (near infrared band) to buildings based on the analysis of various-band spectral information of remote sensing images from ZY-3. The band computational formulas and related information of all other statistics are described in Table 1.

Table 1 Band computational formulas of decision statistics.

Abbreviation	Name	Formula	Remarks
NDWI	Normalized Difference Water index	(G-NIR)/(G+NIR)	G(Green Band), NIR (Near-Infrared Waveband)
NDVI	Normalized Difference Vegetation Index	(NIR-R)/(NIR+R)	R(Red Band)
RVI	Ratio Vegetation Index	NIR/R	
ARVI	Atmospherically Resistant Vegetation Index	[NIR-(2R-B)] /[NIR+2R-B)]	B(Blue Band)
JZZS	Construction Index	B^2-NIR^2	

The sample size of land use types is expanded according to visual interpretation of the high-resolution fused image. Classification rules are determined based on the characteristics analysis of the classification decision statistics of land-use type samples, and the decision-making tree of land-use type classification is set up step by step. The decision-making tree is shown as Fig. 3.

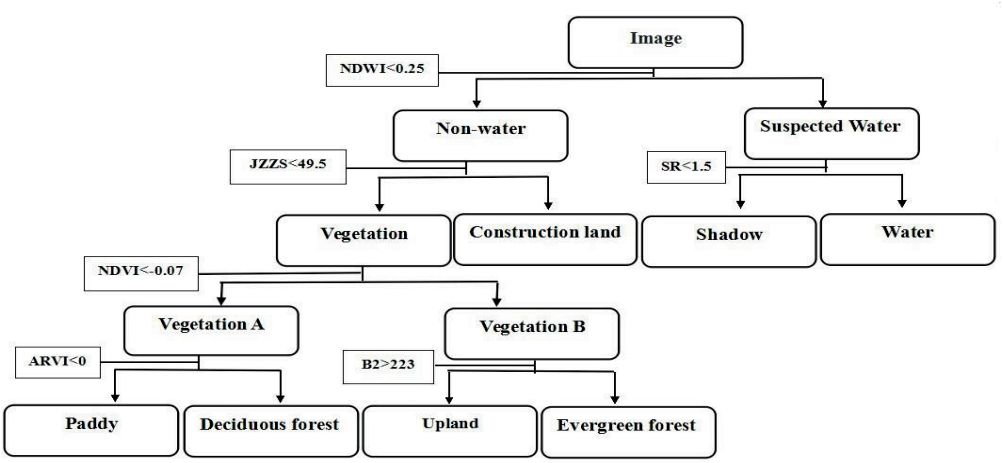

Fig. 3 Decision-making tree of land use type classification (left branch represents yes).

NDVI of the multispectral images on 2 October 2012, 28 January 2013 and 29 July 2013 were extracted, then all NDVI of the multispectral image were synthesized into one as the basis of the construction of the decision-making tree of land-use type classification. The training samples of seven types of land use, such as paddy, upland, evergreen forest, deciduous forest, water body, building land and bare land were selected based on visual interpretation coupled with field investigation. The decision-making tree of land-use type classification is given by use of the CART algorithm to synthesize the NDVI image. According to the decision-making tree of land-use classification got by use of CART algorithm, all land-use types of the watershed were classified.

3.2 Synthesis of the land-use map and accuracy assessment

By use of the decision classification of mono-temporal remote sensing images, the information of evergreen forest, deciduous forest, building land and water body is extracted with better performance. However, the classification information of the paddy, upland and bare land is extracted with poor performance. The cultivated land area obtained from the mono-temporal image is obviously greater than the actual area. Since the experimental watershed has a relatively small area, higher accuracy of land-use type classification is needed for the construction of hydrological models. Consequently, the land-use type classification by use of the slope and height information is obviously not accurate, and could not meet the accuracy requirement of hydrological model. By use of the combined analysis of multiple-temporal images and decision-making tree classification based on the CART algorithm with local farming rules, the information of paddy, upland and bare land is extracted with better performance, and the cultivated land area is consistent with the actual

area. However, the building land area given by use of JZZS of the mono-temporal images decision-making tree is more consistent with the actual case. The final land-use map shown in Fig. 4 was obtained by implanting the water body information extracted by use of the object oriented technology and building land information extracted by use of the mono-temporal decision-making tree classification into the land-use map of the watershed from the multiple-temporal image, with local modifications by comparing it to remote sensing images.

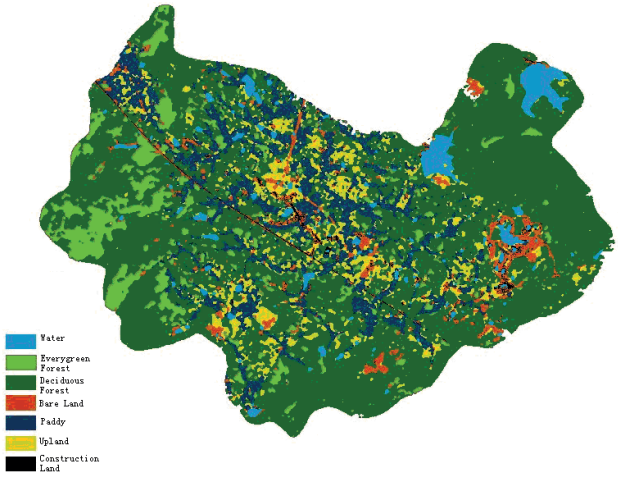

Fig. 4 Land-use map of the Huashan Hydrological Experimental Watershed.

The land use map obtained by interpretation (Fig. 4) was verified by use of visual interpretation of the original remote sensing images. The confusion matrix was established, Kappa coefficient calculated and the accuracy of the final land-use map evaluated.

In total 942 reference samples were obtained by visual interpretation of the original remote sensing images. To ensure the reliability of the reference samples obtained from visual interpretation and the validity of the precision evaluation, the verification samples extracted from reference samples were verified by use of the field validation.

The water bodies could be easily discriminated by visual interpretation of ZY-3 remote-sensing images, and consequently the validation for water body is avoided. Finally, 38 verification samples were randomly selected from the reference samples of six types of land-use data (except water body) for field validation. The land-use types of 38 verification samples obtained from visual interpretation are completely consistent with the actual land-use types, and the reference samples obtained from visual interpretation are reliable. The confusion matrix of the precision evaluation of land-use classification was built (Chen *et al.* 2008), and the result of the precision evaluation is shown in Table 2; the overall classification accuracy was 92.04% and the Kappa coefficient 0.9030.

Table 2 Accuracy assessment of land-use classification.

	Water	Evergreen forest	Deciduous forest	Bare land	Paddy	Upland	Construction land	Raw total
Water	51	0	1	0	0	0	1	53
Evergreen forest	0	153	3	0	5	0	0	161
Deciduous forest	2	1	246	7	3	1	2	262
Bare land	0	0	5	113	4	2	4	128
Paddy	0	2	13	0	156	3	0	174
Upland	0	0	0	2	7	86	1	96
Building land	0	0	2	3	0	1	62	68
Column total	53	156	270	125	175	93	70	942

Overall classification accuracy = 92.04%; Kappa coefficient = 0.9030

4 CONCLUSIONS

In this paper, spatial information of Huashan experimental watershed, such as a DEM and land-use types, is extracted from ZY-3 remote sensing images and studied for digital watershed construction and hydrological simulation. This study has accumulated experience for ZY-3 remote sensing images application in the study of hydrological experimental watersheds.

Water body, as an important research object in hydrological experimental watershed, requires high-accuracy information on the location, number, size and contour in the study of the hydrological experimental watersheds. The water body information is extracted by use of an object-oriented method based on the image spot classification. This method can guarantee a certain accuracy and avoid the "salt and pepper" result.

Land-use types are extracted by the decision tree classification method based on mono-temporal fused images and the multiple-temporal multispectral images. The decision tree classification based on the mono-temporal fused image makes full use of the space feature information, and the decision tree classification based on the multiple-temporal multispectral images makes full use of spectral information. Land-use information from the classification decision tree of the mono-temporal image and multiple-temporal images are optimally synthesized into a final land-use map; the information contained in the remote sensing images has been well utilized.

Acknowledgements This work was supported by Ministry of Water Resources, Special Fund for Scientific Research on Public Causes (201201026).

REFERENCES

Baatz, M. and Schape, A. (1999) Objected-oriented and multi-scale image analysis in semantic networks. *Proc of 2nd international Symposium on Operationalization of Remote Sensing*, Enschede ITC.

Chen, Y. *et. al*. (2008) CART-Based decision tree classifier using multi-feature of image and its application. *Geography and Geo-Information Science* 3, 33−36.

China Centre for Resources Satellite Data and Application (CRESDA) (2012) Introduction of ZY-3. http://www.cresda.com/n16/n1130/n175290/175676.html.

China Centre for Resources Satellite Data and Application (CRESDA) (2013) The radiation calibration coefficients of HJ-1ABZY-3and 02C in 2012 and 2013. http://www.cresda.com/n16/n1115/n1522/n2103/index.html

China Centre for Resources Satellite Data and Application (CRESDA) (2013) The spectral response function. http://www.cresda.com/n16/n1115/n1522/n2118/index.html.

Friedl, M.A., Brodley, C.E., and Strahler, A.H. (1999) Maximizing land cover classification accuracies produced by decision trees at continental to global scales. *IEEE Transactions on Geoscience and Remote Sensin*g 37(2), 969−977.

Fu, C.S. *et al*. (2011) An overview on the water science researches at the experimental watersheds in China and abroad. *Progress In Geography* 30(3), 259−267.

Gu, W.J. *et al*. (2003) Challenges of basin study to traditional hydrological conceptions: the 50 years anniversary of hydrological basin study of PRC and the 20 years anniversary of Chuzhou Hydrological Laboratory. *Advances Inwater Science* 14(3), 368−370.

Han, N.L. *et.al*. (2011) Atmospheric correction of CBERS-02B CCD image based on FLAASH. *Journal of Anhui Agri Sci,* 39(4), 2051−2053.

Li, D.R. *et.al*. (2012) China's first civilian three-line-array stereo mapping satellite: ZY-3. *Acta Geodaetica et Cartographica Sinica* 41(3), 317−322.

Mclver, D.K. and Friedl, M.A. (2002) Using prior probabilities in decision-tree remotely sensed data. *Remote Sensing of Environment* 81, 253−261.

Mclver, D.K. and Friedl, M.A. (2001) Estimating pixel-scale land cover classification confidence using non-parametric machine learning methods. *IEEE Transaction on Geoscience and Remote Sensing* 39, 1959−1968.

Metzler,V.T. and AACT, C. (2002) Object-oriented image analysis by evaluating the causal hierarchy of a partitioned reconstructive scale-space. *Proceeding of ISMM 2002*, CSIRO Publishing.

Wei, X., *et. al.* (2010) Research on land-use classification of Beijing urban area based on decision tree technologies. *2010 International Conference on Remote Sensing* (ICRS).

Wu, J. *et. al*. (2013) Method of earthquake collapsed building information extraction based on high-resolution remote sensing. *Geography and Geo-Information Science* 29(3), 35−38.